Antiviral Research 95 (2012) 118–127

Contents lists available at SciVerse ScienceDirect

Antiviral Research

journal homepage: www.elsevier.com/locate/antiviral

Identification of substituted [3, 2-a] pyrimidines as selective antiviral agents: Molecular modeling study

Kilaru Ravendra Babu [a,f], Valasani Koteswara Rao [a,e], Yellapu Nanda Kumar [b], Kishore Polireddy [c], Kadiam Venkata Subbaiah [d], Matcha Bhaskar [b], Valluru Lokanatha [d], Chamarthi Naga Raju [a,*]

[a] Department of Chemistry, Sri Venkateswara University, Tirupati 517502, India
[b] Division of Animal Biotechnology, Department of Zoology, Sri Venkateswara University, Tirupati 517502, India
[c] Department of Pharmacology, Toxicology and Therapeutics, University of Kansas Medical Center, Kansas City, KS 66160, USA
[d] Department of Biotechnology, Dravidian University, Kuppam 517 425, India
[e] Department of Pharmacology and Toxicology, University of Kansas, Lawrence, KS 66047, USA
[f] Mylan Laboratories Ltd., CRD, Anrich Industrial estate, Bollaram, Jinnaram, Medak 502325, India

ARTICLE INFO

Article history:
Received 29 January 2012
Revised 20 May 2012
Accepted 22 May 2012
Available online 29 May 2012

Keywords:
Antiviral inhibitors
Newcastle disease virus
Dihydropyrimidine
Haemaglutinin–neuraminidase
Molecular modeling

ABSTRACT

A series of novel substituted dihydropyrimidine and 5H-thiazolo [3, 2-a] pyrimidine derivatives were designed and synthesized as a potential target to discover drugs fighting against the viral diseases. The main objective of the present work is to carry out the QSAR studies for all the series of the compounds starting from **4a** to **6j** to find out their molecular descriptors and predict the biological properties. All of them are showing the best QSAR descriptors, hence chosen for the prediction of anti-viral activity against *Newcastle disease virus* (NDV). Initially their inhibitory activity was predicted by molecular docking of these compounds against haemaglutinin–neuraminidase (HN) protein using molecular operating environment (MOE) software. Based on the best affinity and highest docking scores **4b, 5b** and **6b** were assayed *in vivo* on NDV infected chicks and it was found that there is significant improvement in the survival of the chicks with the treatment ($P < 0.05$). **4b** and **6b** showed better curative effect than **5b** at the dose concentration of 40 mg/kg body weight of chicks. The results from molecular docking study and biological assays can be inferred to consider these molecules as potential antiviral drugs.

1. Introduction

Viruses are the small infectious nucleoprotein particles that can replicate and survive only inside the living cells of organisms and can spread many ways. They can infect all types of organisms including humans and are responsible for a wide range of diseases (Breitbart and Rohwer, 2005). Although a number of anti-viral drugs are available, still virus infections remain the major problem to the world due to increasing resistance. Multiple factors such as mutations in the genome, adaptation to new environments, etc., are responsible for the resistance of viruses (Edwards and Rohwer, 2005). Considerable efforts should be devoted to new anti-viral drug discovery for the purpose of improved therapeutic option. Development of new agents with novel structure and mode of action has been particularly hastened providing for emergence of mutant viral antigens and drug resistance. In this context, we have reported a series of dihydropyrimidinone (DHPMs) derivatives which can become promising candidates for anti-viral agents having unique chemical structure. The DHPMs show such broad spectrum of biological activities like antiviral, anticancer (Focher et al., 2000; Sherman and Kaplan, 1975), calcium channel blockers (Eisenberg et al., 2004), antihypertensive agents (Cho et al., 1989), α-1a-antagonists (Bossert and Vater, 1989) and neuropeptide Y (NPY) antagonists (Kappe, 1998, 2000). This activity is due to the presence of dihydropyrimidine core unit.

Herein, we report a simple protocol for the parallel synthesis of DHPMs using appropriate acid catalyst and also the above-cited applications prompted us to synthesize a series of novel pyrimidine derivatives through the reaction of 3,4-dihydropyrimidin-2(1H)-ones (**4**) with 1-bromo-4-phenyl butan-2-ones (**5**) to form the title compounds 5H-thiazolo [3, 2-a] pyrimidine derivatives and evaluation of anti-viral activity of the title compounds. The structures of the newly synthesized compounds (**4a–j**), (**5a–j**) and (**6a–j**) have been established by the elemental analysis and spectral data (IR, ^{1}H, ^{13}C NMR and mass) (Scheme 1).

A QSAR study was carried out for all the series of molecules (**4a–6j**) which can help in early preclinical development and avoid costly late-stage preclinical and clinical failures (Santos et al., 2009; Walters et al., 1999). Three dimensional models can be constructed to analyze the structure based interaction with other biological macromolecules like proteins. The stable confirmation of

* Corresponding author.
E-mail address: rajuchamarthi10@gmail.com (C. Naga Raju).

0166-3542/$ - see front matter © 2012 Elsevier B.V. All rights reserved.
http://dx.doi.org/10.1016/j.antiviral.2012.05.010

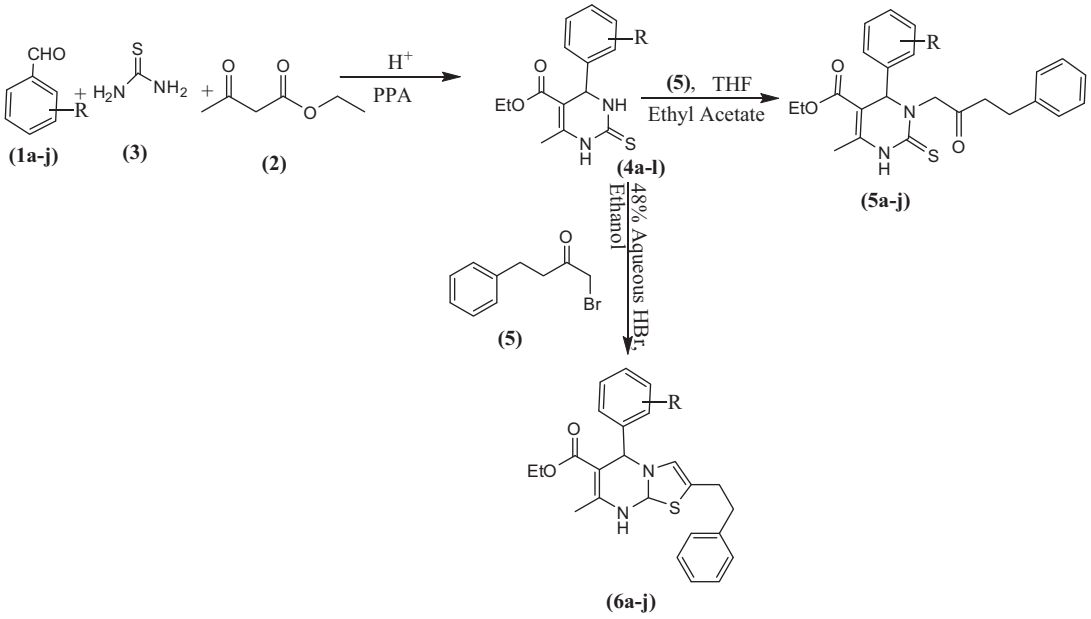

Scheme 1. Synthetic route for the designed target molecules.

the structures can be obtained by molecular dynamics simulations which is an important task to know the behavior of molecule in the system whether in isolated or solvated environment (Kokhan and Shinkarev, 2011).

Three representative molecules were tested for their inhibitory activity against *Newcastle disease virus* (NDV) in chicks which is highly contagious viral disease affecting wild and domestic avian species (Seal et al., 2000). The nucleoprotein (NP), the phosphoprotein (P) and the large polymerase protein (P) form the nucleocapsid, the haemaglutinin–neuraminidase (HN) and fusion (F) proteins constitute the external envelope, and the matrix protein (M) forms the inner layer of the virion. The pathogenicity of NDV is mainly due to the presence of multiple basic amino acids at the cleavage site (Collins et al., 1993). Initially a molecular docking study was carried out on the HN protein of NDV which is the key pathogenic factor (Huang et al., 2004; Ravindra et al., 2008). This study can help to predict the molecular interaction of the compounds with the HN protein, so that their inhibitory activity on NDV could be determined.

To determine the real efficacy of the compounds, an *in vivo* study was conducted for the three compounds (**4b, 5b** and **6b)** that have shown the best less docking score in chick models which are infected with NDV. In general the entry of virus into the host system results in the activation of phagocytes, it may also release prooxidant cytokines such as tumor necrosis factor alpha (TNF-α), interleukin I, soluble neurotoxins, excitatory neurotransmitters and reactive oxygen species (ROS) and reactive nitrogen species (RNS) (Peterhans, 1997). Production of ROS which are free radical derivatives of molecular oxygen and hydrogen peroxide are involved in the damage of various components such as lipids, proteins, carbohydrates, nucleic acids leading to oxidative stress often accompanied by loss of cell function, apoptosis and/or necrosis (Nordberg and Arner, 2001). The ROS are primarily generated by mitochondria, which possess an antioxidant system capable of scavenging by natural cellular defense mechanisms. The antioxidant system comprises of enzymes such as superoxide dismutase (SOD), catalase (CAT), glutathione-*S*-transferase (GST), glutathione peroxidase (GPx) and glutathione molecule under normal conditions (Yu, 1994). ROS have been suggested to be a mediator of cell death induced by a variety of triggers, including viral infection (Schwarz, 1996). In the present study aimed at the mean titer values of hemagglutination and the activity of antioxidant metabolism related enzymes SOD and CAT and lipid peroxidation levels in the liver tissue of NDV infected chicks. The influence of the initial three new drug molecules on the pathogenicity of NDV was studied.

2. Materials and methods

2.1. Chemistry

2.1.1. Synthesis of ethyl 6-methyl-4-(3-nitrophenyl)-2-thioxo-1, 2, 3, 4-tetrahydro- pyrimidine-5-carboxylate (4b)

A solution of ethyl acetoacetate (510 mg, 3.9 mmol), 3-nitro benzaldehyde (500 mg, 3.3 mmol) and thiourea (300 mg, 3.9 mmol) in ethanol (5 mL) was heated under reflux (78–80 °C) in the presence of poly phosphoric acid (1110 mg, 3.3 mol%) for 12 h under nitrogen atmosphere. The progress of the reaction was monitored by TLC (hexane: ethyl acetate, 1:1 v/v). The reaction mixture, after being concentrated under vacuum at 50 °C, cooled to room temperature, it was poured into crushed ice (10 g) and stirred for 5–10 min. The solid separated was filtered under suction, washed with ice-cold water (20 mL) and then recrystallized from hot ethanol to afford pure product (900 mg, 90%), mp 206–207 °C (lit. mp 206–207 °C). R_f 0.37; (hexane: ethyl acetate, 1:1 v/v). Yield: 82%; IR: 3179, 2988, 2676, 1715, 1660, 1595, 1532, 1475, 1376, 1344, 1325, 1275, 1190, 1130, 1102, 1038, 1015, 906, 889, 871, 808, 786, 737, 689, 650, 508 cm^{-1}; ^1H NMR (DMSO–d_6) δ 1.12 (*t*, 3H), 2.36 (*s*, 3H), 3.98–4.14 (m, 2H), 5.40 (*d*, *J* = 7.4 1H), 7.69–7.76 (m, 2H), 8.13–8.21(m, 2H), 9.83 (*s*, 1H), 10.5 (*s*, 1H); ^{13}C NMR (DMSO–d_6) δ 13.87, 17.18, 53.4, 59.7, 99.8, 121.1, 122.6, 130.3, 132.9, 145.4, 145.9, 147.7, 164.8, 174.5; LCMS m/z (%): 322 [MH^+ 100%]; Anal. Calcd. $C_{14}H_{15}N_3O_4S$: C, 52.33; H, 4.70; N, 13.08; Found: C, 52.26; H, 4.67; N, 13.04.

2.1.2. Synthesis of ethyl 6-methyl-4-(3-nitrophenyl)-3-(2-oxo-4-phenylbutyl)-2-thioxo-1, 2, 3, 4-tetrahydropyrimidine-5-carboxylate (5b)

Ethyl 6-methyl-4-(3-nitrophenyl)-2-thioxo-1,2,3,4-tetrahydropyrimidine-5-carboxylate (500 mg, 1.5 mmol), ethyl acetate (2.5 mL), and tetrahydrofuran (2.5 mL)were taken into three

necked round bottom flask and cooled to 0–5 °C, then 1-bromo-4-phenylbutan-2-one (370 mg, 1.6 mmol) was added, and the reaction mixture was stirred for 20 h. Progress of the reaction was monitored by TLC (hexane: ethylacetate1:1), and the white solid formed was filtered off and washed with chilled ethyl acetate, solid was dried under vacuum at 70 °C to get the pure product (600 mg, 83%). R_f 0.42; (hexanes: ethyl acetate, 1:1 v/v). Yield: 78%; m.p.196–198 °C; IR: 3235, 3108, 2796, 1715, 1668, 1569, 1527, 1348, 1322, 1301, 1278, 1254, 1195, 1146, 1092, 1055, 1030, 963, 873, 740, 699, 639, 609, 588, 520 cm^{-1}; ^1H NMR (DMSO–d_6) δ 1.08 (*t*, 3H), 2.23 (*s*, 3H), 2.26–2.77 (m, 4H), 3.34–3.56 (m, 2H), 3.92–4.10 (m, 3H), 6.87–6.90 (m, 1H), 7.04–7.38 (m, 5H), 7.59–7.85 (m, 2H), 8.08–8.15 (m, 2H); ^{13}C NMR (DMSO–d_6) δ 14.2, 17.3, 28.9, 36.7, 37.9, 54.5, 60.7, 66.9, 99.5, 100.5, 122.2, 123.4, 126.5, 128.3, 130.7, 133.8, 140.0, 142.8, 143.6, 147.4, 163.4, 166.6. LCMS m/z (%): 468 [MH^+ 100%]; Anal. Calcd. $C_{24}H_{25}N_3O_5S$: C, 61.65; H, 5.39; N, 8.99; Found: C, 61.59; H, 5.34; N, 8.95.

2.1.3. Synthesis of ethyl 7-methyl-5-(3-nitrophenyl)-2-phenethyl-5H-thiazolo [3, 2-a] pyrimidine-6-carboxylate (6b)

Ethyl 6-methyl-4-(3-nitrophenyl)-3-(2-oxo-4-phenylbutyl)-2-thioxo-1,2,3,4-tetrahydro pyrimidine-5-carboxylate **5b** (500 mg,1.5 mmol), ethyl acetate (2.5 mL), 1-bromo-4-phenylbutan-2-one (370 mg, 1.6 mmol), 48% aqueous hydrobromic acid (155 mg, 1.5 mmol) and ethanol (5 mL) were taken into three necked round bottom flask and refluxed with stirring for 3 h, the progress of the reaction was monitored by TLC, solvent was removed under vacuum at 50 °C, solid obtained was taken into distilled water (10 mL) extracted with dichloro methane (20 mL), solvent was removed under vacuum at 50 °C, solid was recrystallized from ethanol to get white solid (600 mg, 85%). m.p. 182–184 °C. R_f 0.5; (hexane: ethyl acetate, 1:1 v/v). Yield: 71%; m.p.182–184 °C; IR: 3432, 2975, 2939, 2879, 2802, 2739, 2677, 2602, 2529, 2491, 2238, 2134, 1902, 1687, 1596, 1531, 1476, 1434, 1397, 1384, 1289, 1272, 1256, 1186, 1171, 1070, 1036, 904, 849, 805, 759 cm^{-1}; ^1H NMR (DMSO–d_6) δ 1.04 (*t*, 3H), 2.21 (*s*, 3H), 2.42–2.64 (m, 3H), 2.89–2.98 (m, 1H), 3.85–3.99 (m, 2H), 6.46 (s, 1H), 6.85–7.09 (m, 6H), 7.45–7.66 (m, 2H), 7.99–8.14 (m, 2H); ^{13}C NMR (DMSO–d_6) δ 13.8, 15.1, 23.1, 27.2, 32.5, 57.6, 60.7, 61.2, 101.1, 109.1, 122.1, 124.1, 126.2, 128.3, 131.6, 139.3, 140.6, 141.5, 143.3, 147.7, 161.1, 163.6. LCMS m/z (%): 450 [MH^+ 92%]; Anal. Calcd.$C_{24}H_{23}ClN_2O_2S$: C, 65.67; H, 5.28; N, 6.38; Found: C, 65.62; H, 5.23; N, 6.34.

The same experimental procedure was adopted for the preparation of the remaining title compounds (**6a, 6c–j**).

2.2. Molecular docking of HN protein

The ligand study was carried out by HyperChem software which is a sophisticated molecular modeling environment that uniting with quantum chemical calculations, molecular mechanics, and dynamics (Dastmalchi et al., 2008). Three-dimensional structures were constructed and optimized for all the molecules. QSAR descriptors were studied followed by Lipinski rule filtration. Molecular dynamics simulations were carried out by solvating the structures with water molecules in AMBER force field and the stabilized confirmations were saved (Sippl, 2002).

Docking studies have been performed using MOE 2008.10. The crystal structure of HN protein (PDB ID: 1USX) was retrieved from Protein Data Bank (http://www.rcsb.org/pdb/home/home.do) (Kumar et al., 2005). In order to prepare the protein for docking studies, it is loaded into MOE and all water molecules and hetero atoms were removed. As the protein is a homo trimer consisting of A, B and C chains, chain A was considered for docking process. The structure is protonated, polar hydrogens were added and energy minimization was carried out to get the stabilized conformation. The active site was identified from PDBSum and also correlated with 'Site Finder' module of MOE to define the docking site for the ligands. A ligand data base has been developed for all the compounds to proceed for docking. Docking procedure was followed using the standard protocol implemented in MOE 2008.10. After the successful docking process, the best energy conformations of receptor–ligand complexes were studied and evaluated to infer the affinity levels of all the ligands.

2.3. Pharmacology

2.3.1. Procurement and maintenance of experimental animals

Day old male layer specific pathogen free (SPF) chicks (35 ± 5 g) were selected as experimental animals. The chicks were purchased from Balaji Hatcheries Pvt. Ltd., Chittoor, AP. Animals were held in separate isolators with free access to food and water in an air-conditioned environment (25 ± 2 °C) with a 12 h light and 12 h dark cycle. The experiments were carried out in accordance with the guidelines of the Committee for the Purpose of Control and Supervision on Experiments on Animals, Government of India (CPCSEA, 2003) and approved by the Animal Ethical Committee at Sri Venkateswara University, Tirupati, India (vide No. 04/a/CPCSEA/IAEC/08–09/ZOOL/WR/dated 01.09.2009) (Schwarz, 1996).

2.3.2. Virus

The mesogenic strain of *Newcastle disease virus* (NDV) was obtained from Department of Microbiology, Sri Venkateswara Veterinary University, Tirupati; A.P. Virus titers of the NDV were determined by inoculating chick embryonating eggs and calculated median egg infectious (EID_{50}) by the method of Armitage (Armitage and Allen, 1950) EID_{50} was found to be 10^{-2} (Ohkawa et al., 1979). This virus stock was stored at −40 °C until use.

2.3.3. Haemagglutination test

Serial twofold dilutions of each viral preparation were made in 0.01 M PBS, using 50 μL volumes in V-shaped 96-well micro titer plates. 50 μL of 0.5% suspension of chick red blood cells (RBCs) were added to each well of the plates. The contents in plates were mixed with a mechanical vibrator. The plates were incubated at room temperature (22–25 °C) until the cell control showed complete setting of RBCs. The haemagglutination titer (HA titer) was the reciprocal of the dilution of virus in the last well with complete haemagglutination.

2.3.4. Assay of antioxidants and antioxidant enzymes

Selected biochemical constituents and enzymes representing antioxidant metabolism were estimated in selected tissues of control and experimental chicks. MDA levels were estimated according to the method of Hiroshi et al. (Misra and Fridovich, 1972; Ohkawa et al., 1979). The activity of superoxide dismutase (SOD) was assayed by the method of (Misra and Fridovich, 1972; Ohkawa et al., 1979) catalase (CAT) activity was estimated by the method of Kar (Kar and Mishra, 1976).

2.3.5. Histopathological examination

At the time of slaughtering, liver tissue was isolated and immediately fixed in 10% buffered formalin. Fixed tissues were processed by dehydration and paraffin embedding. Five micrometer sections were stained with hematoxylin and eosin (H&E) and histological changes were observed under the light microscope.

2.3.6. Protein estimation

Protein content was determined following the method of Lowry (Morton and Evans, 1992; Ohkawa et al., 1979) using bovine serum albumin as a reference standard.

Table 1
Representative compounds.

Entry	R	Time (min)/Yield (%)[a]	M.P. (°C)[b]	
			Found	Reported
4a	H	17/95	204–205	205–206 (Walters et al., 1999)
4b	3-No_2	17/95	206–207	206–207 (Santos et al., 2009)
4c	2-No_2	17/95	133–134	-
4d	3-OMe	15/92	128–130	150–152 (Kokhan and Shinkarev, 2011)
4e	3-Cl	16/82	197–199	196–198 (Seal et al., 2000)
4f	4-F	20/90	183–184	184 (Collins et al., 1993)
4g	3,4-OMe	18/87	164–165	165–166 (Huang et al., 2004)
4h	4-Me	18/87	172–174	172–174 (Ravindra et al., 2008)
4i	3-OH	18/87	185–187	184–186 (Peterhans, 1997)
4j	4-OMe	18/87	239–240	240–242 (Santos et al., 2009)

[a] Isolated yields.
[b] All the melting points were matched with the reported data.

3. Results and discussion

3.1. Chemistry

3-Nitro benzaldehyde **1b**, ethyl acetoacetate **2** and thiourea **3** were taken in ethanol and heated under reflux in the presence of poly phosphoric acid (3.3 mol%) for 12 h to yield dihydropyrimidine derivative **4b.** The compound **4b** was taken in an equal molar ratio of ethylacetate in THF and cooled to 0–5 °C, then 1-bromo-4-phenylbutan-2-one **5**, was added and the reaction mixture was stirred for 20 h to obtain the title compound **5b**, where as the compound **4b** when treated with 1-bromo-4-phenylbutan-2-one in presence of aqueous HBr (48%) in ethanol under reflux for 3 h to obtain the title compound **6b** (Scheme 1, Tables 1 and 2).

The chemical structures of all the title compounds **4a–j**, **5a–j** and **6a–j** were characterized by IR, ^1H, ^{13}C NMR and APCI–MS studies and their data are presented in the experimental section. Characteristic IR stretching absorptions were observed in the regions 3144–3275 cm^{-1} and 3568–3365 cm^{-1} for N–H (Kumar et al., 2006), O–H (Khandazhinskaya et al., 2002) respectively. The ester carbonyl stretching frequency was observed in the range of 1715–1745 cm^{-1} (Rao et al., 2011). In the ^1H NMR spectra of title compounds **4d, 4e, 5d** and **5e**, the chemical shifts of aromatic hydrogens of the phenyl ring appeared as multiplets in the region δ 7.54–7.88 (Han et al., 1992; Rao et al., 2010, 2011). The N–H proton resonated as a broad singlet in the region δ 9.25–10.52 (Rajanarendar et al., 2010).The OH protons were observed as singlets in the region 8.52–11.34 ppm. ^{13}C NMR chemical shifts for title compounds were observed in their expected regions.

3.2. QSAR study

Three-dimensional structures were built for all the compounds ranging from **4a** to **6j** and optimized by using Hyper Chem software. Molecular dynamics simulations were carried out and molecular descriptors were determined by QSAR study and Lipinski rule and the results showing that all molecules have drug like properties (Table 3). All the compounds have the molecular weight less than 500 Da except **6c** which is showing a molecular weight of 541.54 D and **4a** has the lowest molecular weight of 276.35 Da. All the compounds are showing hydrogen bond donors and hydrogen bond acceptors less than 5 and 10 respectively and finally the log *P* values of these compounds are superior to act as drug which is less than 5. Molar refractivity is also in the range of 40–130. QSAR study is a powerful lead optimization tool that can quantitatively relate variations in biological activity to changes in molecular properties. The molecular descriptors of the present molecules are in optimal ranges and log *P* value that indicates the absorption and solubility were not exceeded the limited value of 5.

Table 2
Representative compounds.

Entry	R	Entry	R
5a and **6a**	H	**5f** and **6f**	4-F
5b and **6b**	3-No_2	**5g** and **6g**	3,4-OMe
5c and **6c**	2-No_2	**5h** and **6h**	4-Me
5d and **6d**	3-OMe	**5i** and **6i**	3-OH
5e and **6e**	3-Cl	**5j** and **6j**	4-OMe

3.3. Molecular docking of HN protein

The crystal structure of HN protein was loaded into MOE (Molecular Operating Environment (MOE, version 2002.03) (2002) with a resolution of 2.70 Å and a library was constructed for all the lead molecules (Davies et al., 2011). The binding site of 2-deoxy-2,3-dehydro-*n*-acetyl-neuraminic acid (DAN) on HN protein was identified from PDBSum (Laskowski, 2001) and the residues Arg 174, Glu 258, Tyr 299, Tyr 317, Arg 363, Glu 401, Arg 416, Val 466, Arg 498 and Tyr 526 were found to be interacting with DAN. The site finder module of the MOE was used to identify the additional ligand binding sites within the protein structure. Hydrophobic and hydrophilic spheres are used to identify the interactive positions which will be potential ligand binding sites in the each possible position. Among the group of binding sites generated by site finder module, the centroid sphere of site 4 was selected which also includes the residues of DAN binding site. All the dummy atoms were matched for centroid sphere of site 4 during the characterization of ligand binding site.

Docking simulations were performed with MOE-dock system using the ligand data base generated for all the series of leads. A total of 30 most favorable binding sites and orientations were generated for each lead molecule. The affinity scoring function δG was used to assess and rank the receptor–ligand complexes. The ligand poses were also scored within the centroid sphere of binding pocket. The docking scores of all the lead molecules and their hydrogen bonding strength were tabulated and shown in Table 4.

Among all docking conformations, **5b** is showing best least docking score of −20.471 and the next best least docking score is found with **4b** followed by **6b**. **5b** is found to be forming two hydrogen bonds of lengths 2.6 and 2.7 Å each with Asp278 and Gln280 respectively. The –OH group of the ligand is interacting with the –COOH group of Gln280 and amino nitrogen of heterocyclic ring of ligand is interacting with –COOH group of the Asp278 (Fig. 2). **4b** is forming only a single hydrogen bond of 2.7 Å using double bonded oxygen atom with –OH group of hydroxy benzene ring of Tyr262. This ligand is also making a solvent contact with

Table 3
Molecular descriptors of substituted thiazolo [3, 2-a] pyrimidine derivatives from QSAR study.

Ligand	Molecular weight (Da)	Hydrogen bond donors	Hydrogen bond acceptors	Log *P*	Molar refractivity (A^{o3})	Surface area (A^{o2})	Volume (A^{o3})	Hydration energy (K.cal/mol)	Polarizability (A^{o3})	Gradient energy (K.cal/molA^{o})	Total energy (K.cal/mol)
4a	276.35	2	4	1.73	43.64	453.14	837.28	−8.51	30.82	0.097	63.964
4b	321.35	2	6	1.7	49.64	481.02	887.67	−12.77	32.53	0.096	66.525
4c	321.35	2	6	2	42.53	442.48	868.73	−10.06	49.64	0.096	67.727
4d	306.38	2	5	1.70	50.06	521.30	887.45	−8.60	33.29	0.0988	72.303
4e	287.36	2	4	1.98	42.75	370.48	832.60	−8.01	30.43	0.0874	60.2325
4f	294.34	2	5	2.02	43.55	427.73	825.48	−7.74	30.73	0.08745	59.298
4 g	336.41	2	6	3.65	56.49	509.33	957.20	−10.18	35.76	0.0977	78.592
4 h	290.38	2	4	2.12	48.25	436.40	839.09	−7.66	32.65	0.09917	69.3137
4i	292.35	3	5	1.75	45.03	402.84	818.60	−13.55	31.46	0.0995	64.0868
4j	306.38	2	5	1.07	50.06	502.75	908.98	−9.41	33.29	0.0959	71.443
5a	422.54	1	5	3.64	63.72	618.60	1234.43	−6.91	47.91	0.0972	101.788
5b	467.54	1	7	2.99	69.72	597.82	1242.03	−13.66	49.62	0.3311	1236.99
5c	467.54	1	7	3.82	69.72	647.96	1273.74	−10.98	49.62	0.0984	110.224
5d	452.57	1	6	3.82	70.14	640.44	1272.70	−8.82	50.38	0.0960	111.233
5e	433.54	1	5	3.98	62.83	489.42	1192.10	−8.11	47.52	0.0953	1234.9
5f	440.53	1	6	4.14	63.63	612.29	1228.04	−7.02	47.81	0.09243	99.5773
5 g	482.59	1	7	4.83	76.57	643.33	1349.29	−9.96	52.85	0.2088	1251.36
5 h	436.57	1	5	3.88	68.33	553.88	1236.09	−7.39	49.74	0.2818	1238.49
5i	438.54	2	6	2.69	65.11	558.24	1202.15	−11.58	48.54	0.0984	98.773
5j	452.57	1	6	4.17	70.14	675.02	1309.31	−8.54	50.38	0.0894	111.891
6a	406.54	1	4	4.86	59.65	570.31	1174.20	−5.47	46.61	0.0939	114.416
6b	451.54	1	6	4.84	65.64	631.07	1258.98	−11.54	48.32	0.09237	117.088
6c	541.54	1	6	4.46	65.64	464.77	1148.48	−5.79	48.32	0.09106	119.364
6d	436.57	1	5	4.84	66.07	613.42	1251.22	−6.07	49.08	0.0963	116.287
6e	417.55	1	4	4.82	58.75	567.85	1236.81	−4.86	46.22	0.0995	114.011
6f	424.53	1	5	4.16	59.55	623.86	1220.50	−5.38	46.52	0.0948	112.613
6 g	466.59	1	6	4.62	72.49	691.73	1351.47	−7.85	51.55	0.0922	132.001
6 h	420.57	1	4	4.25	64.25	640.25	1244.63	−4.62	48.44	0.0906	120.196
6i	422.54	2	5	4.88	61.01	559.01	1201.10	−10.72	47.24	0.0908	113.005
6j	436.57	1	5	4.64	66.07	657.39	1283.93	−6.85	49.08	0.0943	122.092

Table 4
Docking interactions substituted thiazolo [3, 2-a] pyrimidine derivatives.

Ligand[a]	Docking score[b]	No. of hydrogen bonds with binding site[c]
4a	−12.378	0
4b	−19.271	1
4c	−12.212	4
4d	−14.060	0
4e	−14.404	0
4f	−14.205	0
4g	−15.491	1
4h	−13.489	0
4i	−18.817	0
4j	−16.005	2
5a	−9.216	2
5b	−20.471	2
5c	−10.478	1
5d	−12.612	0
5e	−11.280	0
5f	−10.068	0
5g	−12.201	0
5h	−11.605	1
5i	−10.459	0
5j	−9.766	1
6a	−11.729	1
6b	−19.195	1
6c	−18.202	4
6d	−12.826	1
6e	−12.541	0
6f	−12.585	1
6g	−13.131	3
6h	−11.338	1
6i	−12.931	0
6j	−9.460	1

[a] The novel thiazolo [3, 2-a] pyrimidine derivatives.
[b] Docking scores generated during MOE docking between the novel leads and HN protein binding domain.
[c] Number of hydrogen bonds formed between the HN protein binding domain and the novel leads.

Arg 363 (Fig. 3). **6b** is also forming a single hydrogen bond of 2.6 Å with the help of one of the nitrogen atom of hetero cyclic ring of ligand with –COOH group of Asp143 (Fig. 4). These three ligands are showing first best least docking scores with stable ligand pose interactions in the docking sphere followed by the remaining lead compounds.

3.4. Biological activity

After synthesis, QSAR and molecular docking studies, further experiments were carried out with **4b**, **5b** and **6b** as they showed best docking scores among all the leads. *In vivo* assays were conducted and evaluated to check whether these three compounds have therapeutic potential or not. To achieve this task, two studies were performed. Firstly, *in vivo* screening of these compounds in NDV infected chickens for antiviral activity and secondly, pro- and anti-oxidant enzyme status in the liver of the same. Hemagglutination (HA) titers were significantly increased in NDV-infected animals as compared to control animals on 10 days of post infection on the other hand the HA titers were significantly ($P < 0.001$) decreased in NDV+compound **4b** and NDV+compound **6b** treated group animals and slightly in NDV+compound **5b** treated animals (Fig. 1). A significant ($P < 0.05$) increase was observed in the survival rates of NDV infected and compounds (**4b** and **5b)** treated animals when compared to NDV-infected animals (Fig. 5). A significant increase was observed in the levels of lipid peroxidation (Fig. 6) and depletion in the activity levels of catalase (Fig. 7) and superoxide dismutase (Fig. 8) in the liver tissue of NDV infected chicks. Interestingly the chicks treated with compounds **4b** and **6b** significantly ($P < 0.001$) decreased MDA levels and improved the antioxidant enzyme activities in liver tissue of chicks compared to NDV infected animals.

The histological alterations like intense vacuolar degeneration of hepatocytes and focal coagulation necrosis of parenchyma and relapse of hepatocytes were observed in the liver of NDV infected chicks. On the other hand, the lesions in the liver of NDV infected chickens were reduced after injection of drugs **4b** and **6b** over virus alone infected chickens (Fig. 9). Whereas, injection of **5b** into NDV infected chicks showed mild necrosis in the liver.

The results clearly demonstrated that the therapeutic concentrations of compounds **4b** and **6b** at 20 or 40 mg/kg body weight inhibited the viral concentrations as evidenced by significant ($P < 0.05$) decrease in the mean titers of the hemagglutination. Further, an inverse correlation was observed between the concentration of the compounds (**4b** and **6b**) and the mean titers of hemagglutination, suggesting that higher concentrations of the compounds **4b** and **6b** (40 mg/kg bw) were very effective in inhibiting the virus concentrations. However, injection of **5b** at 20 or 40 mg/kg bw was unable to elicit such antiviral response.

The content of malondialdehyde levels, an indicator of lipid peroxidation was significantly increased in the liver of chicks exposed to NDV. This increase in the lipid peroxidation products were accompanied by a significant decrease in the activity levels of superoxide dismutase and catalase. This clearly indicates that NDV-mediated infection affects pro-and anti-oxidant balance in the liver of chicks. Earlier, it has been reported that influenza virus induces oxidative stress as evidenced by accumulation of lipid

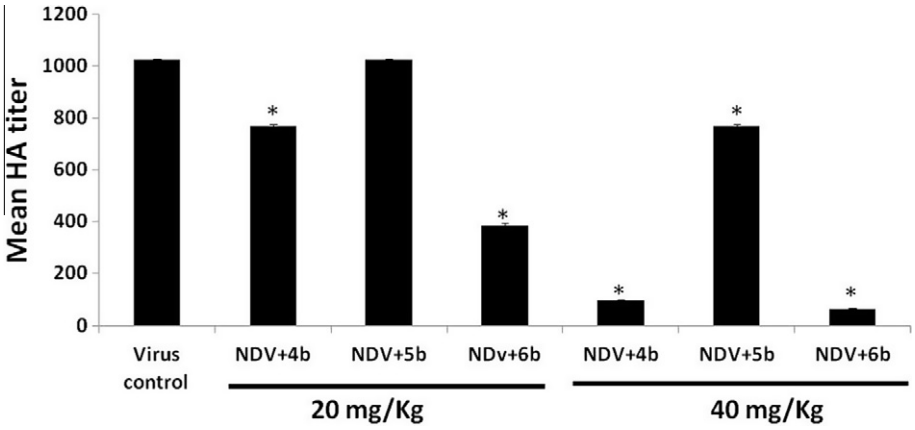

Fig. 1. Mean of haemagglutination titers after the inoculation of chicks with *Newcastle disease virus* and the administration of synthesized chemical candidates (**4b**, **5b** and **6b**) after virus infection. *Indicates significantly different from virus control group ($P < 0.05$).

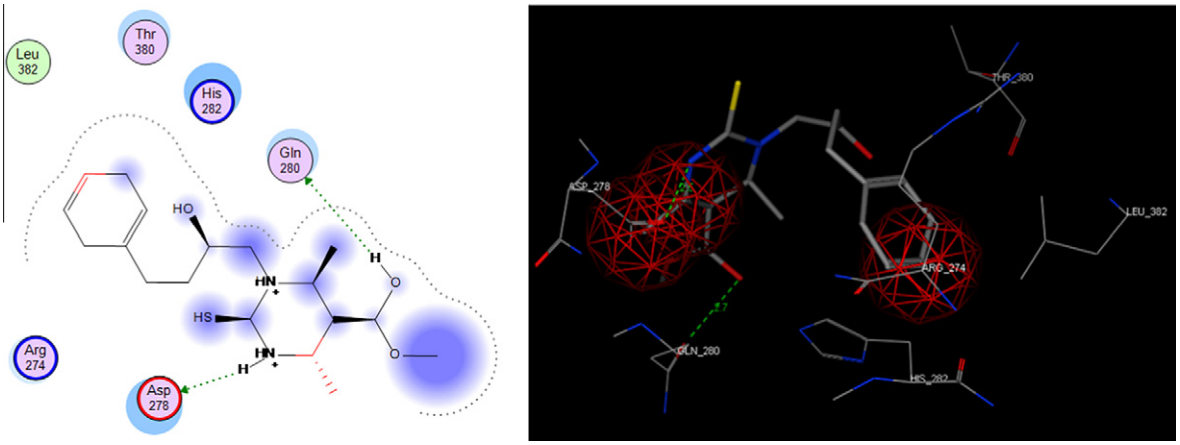

Fig. 2. Interaction of **5b** with binding site of HN protein.

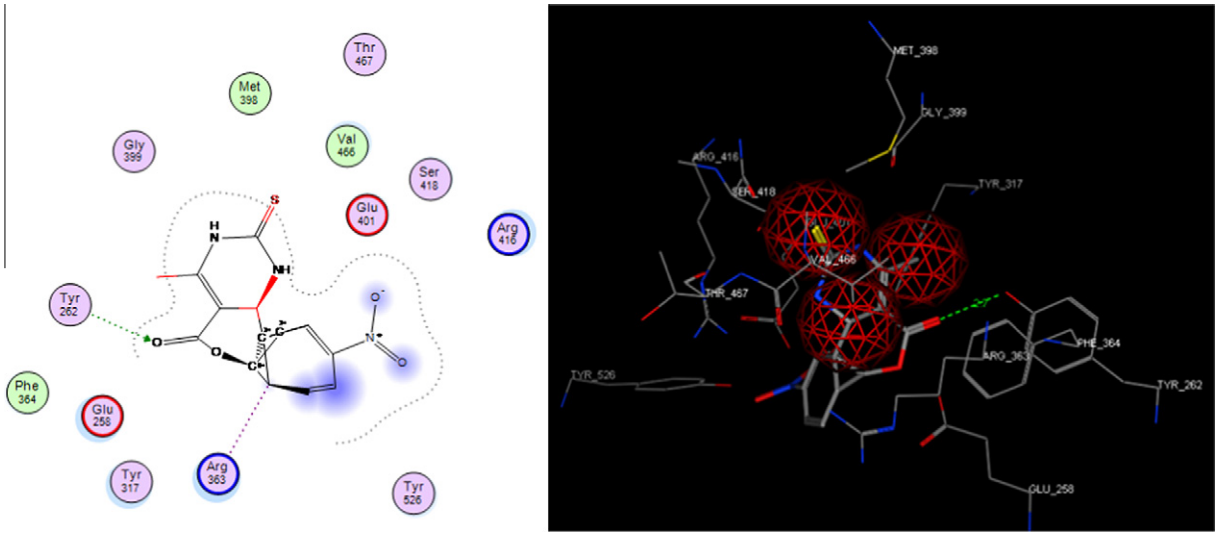

Fig. 3. Interaction of **4b** with binding site of HN protein.

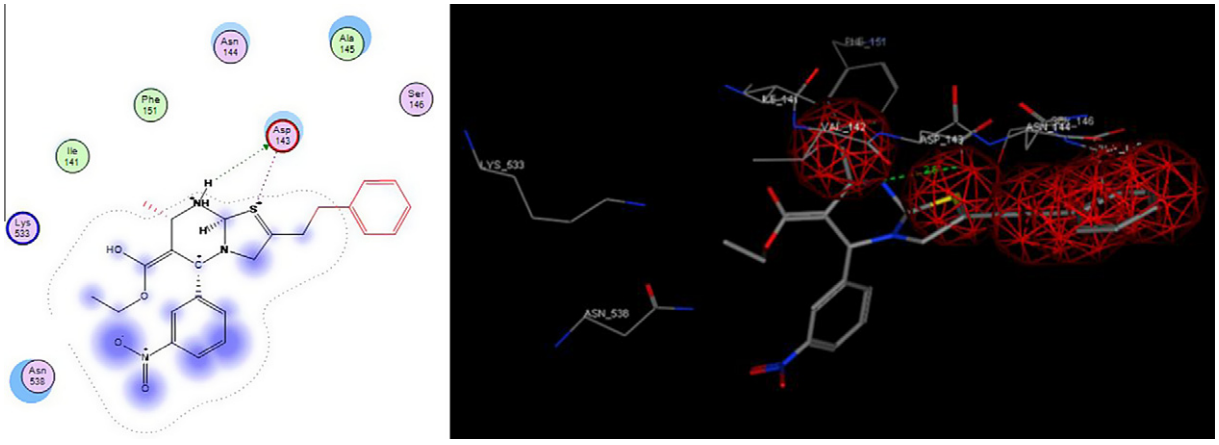

Fig. 4. Interaction of **6b** with binding site of HN protein.

peroxidation products in the blood and lung of animal models leading to tissue injury (Kornbrust and Mavis, 1980).

It is well established that an intrinsic antioxidant mechanism is involved to protect the cells/tissues from ROS-induced damage or to check their levels within normal limits. Under physiological conditions, superoxide dismutase (SOD) is believed to be the first line of antioxidant enzyme which converts ROS, the superoxide anion, into hydrogen peroxide and molecular oxygen and the resulting

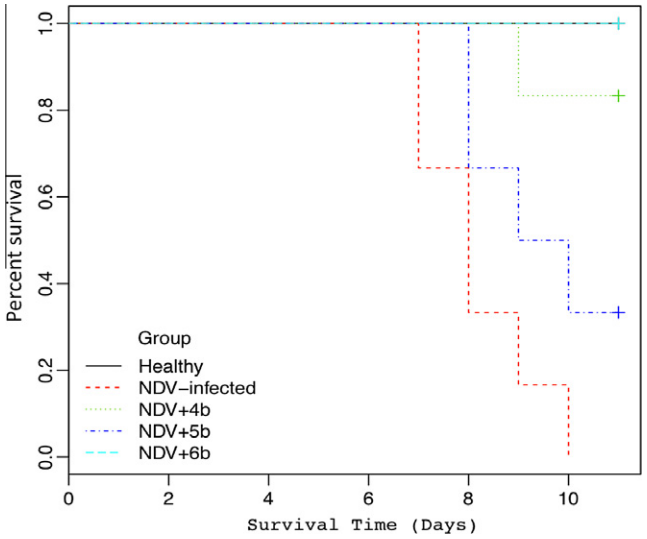

Fig. 5. Survival analysis of NDV infected chicks after treatment with the title compounds **4b**, **5b**, **6b**: Kaplan–Meier estimates of survival between healthy, NDV infected, and treatment groups. Log-rank comparisons revealed that title compounds **4b** and **6b** increased the survival time of NDV infected chicks (log-rank; $\chi^2 = 27.7$, $P = 1.47E{-}0.5$).

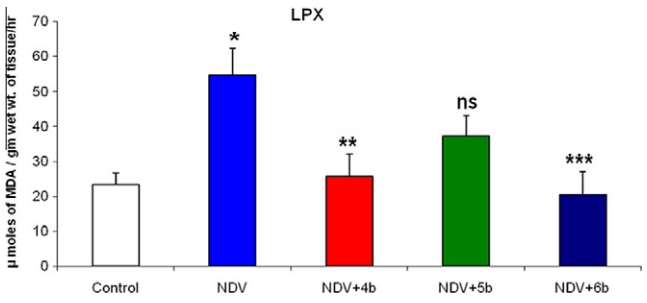

Fig. 6. Bar graph showing malonaldehyde levels in liver of control, NDV-infected and NDV+compounds (**4b**, **5b** and **6b**) treated chicks. All values are expressed as mean±S.D of six individual observations. $^{*}P < 0.05$ between control group and NDV-infected group, $^{**}P < 0.05$ between NDV-infected group and NDV+**4b** treated group, $^{***}P < 0.001$ between NDV-infected group and **6b** treated group, ns = non significant.

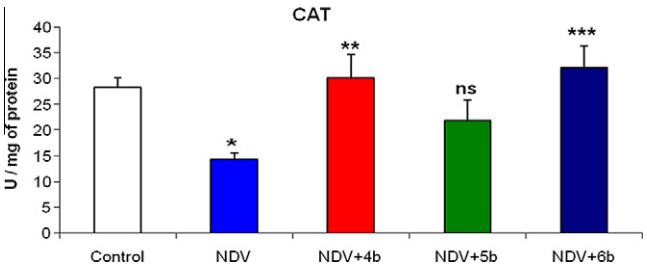

Fig. 7. Bar graph showing activity levels of catalase in liver of control, NDV-infected and NDV+compounds (**4b**, **5b** and **6b**) treated chicks. All values are expressed as mean±S.D of six individual observations. $^{*}P < 0.05$ between control group and NDV-infected group, $^{**}P < 0.05$ between NDV-infected group and NDV+**4b** treated group, $^{***}P < 0.001$ between NDV-infected group and **6b** treated group, ns = non significant.

hydrogen peroxide is converted to water by the enzyme catalase (Halliwell and Gutteridge, 1985). In the present study, the activity of SOD was significantly lowered in liver of NDV-infected chicks when compared with the control animals. This may lead to the accumulation of singlet oxygen and hydroxyl radicals in the immediate environment which in turn may be responsible for the

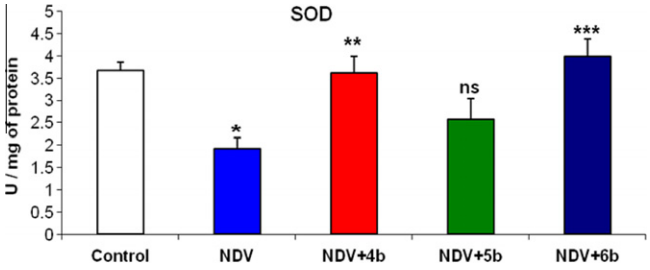

Fig. 8. Bar graph showing activity levels of superoxide dismutase in liver of control, NDV-infected and NDV+compounds (**4b**, **5b** and **6b**) treated chicks. All values are expressed as mean±S.D of six individual observations. $^{*}P < 0.05$ between control group and NDV-infected group, $^{**}P < 0.05$ between NDV-infected group and NDV+**4b** treated group, $^{***}P < 0.001$ between NDV-infected group and **6b** treated group, ns = non significant.

decline in the activity of SOD observed in the present study. Consistent with our results, it also reported (Kumar et al., 2005) that decreased SOD activity levels in mice infected with influenza virus. Further, the decreased activities of catalase in virus infected tissues of birds over control chicks may indicate the accumulation of hydrogen peroxide. However, treatment of compounds **4b** and **6b** were significantly ($P < 0.05$) increased the activity levels of antioxidant enzymes like SOD and CAT in the liver tissue. Since, catalase protects SOD inactivation by H_2O_2, while the SOD reciprocally protects catalase against inhibition by superoxide anion. Thus, a balance of the activities of these enzyme systems may be essential to eliminate superoxide and peroxide radicals generated in the tissues. The treatment of **4b** and **6b** to NDV infected chicks sustains the balanced circuit of SOD/catalase in the liver and as a result increases the activity levels of both enzymes.

The histological alterations like intense vacuolar degeneration of hepatocytes and also in the live parenchyma in the liver was observed in the NDV infected tissues over a period of 10 days. On the other hand, these histological alterations were restored to normal status in compounds like **4b** and **6b** treated virus infected liver of chicks (Fig. 8). It is evident from these studies that increased generation of free radicals are responsible for tissue damage (Machlin and Bendich, 1987) during virus infection as evidenced by increased lipid peroxidation products accompanied by poor antioxidant enzyme status. Whereas, compounds like **4b** and **6b** treatment in virus infected chicks alleviates the activity levels of antioxidant enzymes which in turn combat the lipid peroxidation products to protect tissues from free-radical injury. Nevertheless, further experiments are required to elucidate the mechanism of action for these compounds.

In conclusion the molecular descriptors of three molecules explained their drug likeliness and their usefulness as drugs. The molecules with the optimum parameter values obtained in QSAR study will not affect the host system, but acts against pathogens like virus. All the docking scores and hydrogen bond interactions of three compounds with HN protein encouraging them as good antiviral drugs which in turn strengthen by their QSAR study. In addition, the results from biological assay of three molecules in NDV infected chicks giving experimental support for their anti-viral activity. Thus with the best binding energies, good hydrogen bond interactions and less toxicity ensures **4b, 5b** and **6b** molecules as antiviral agents and can be promoted for further drug development stages.

3.5. Statistical analysis

The data were analyzed using a statistical package for social sciences (SPSS, 11.5 versions). A one way ANOVA was performed followed by Tukey multiple comparisons test, for comparison of

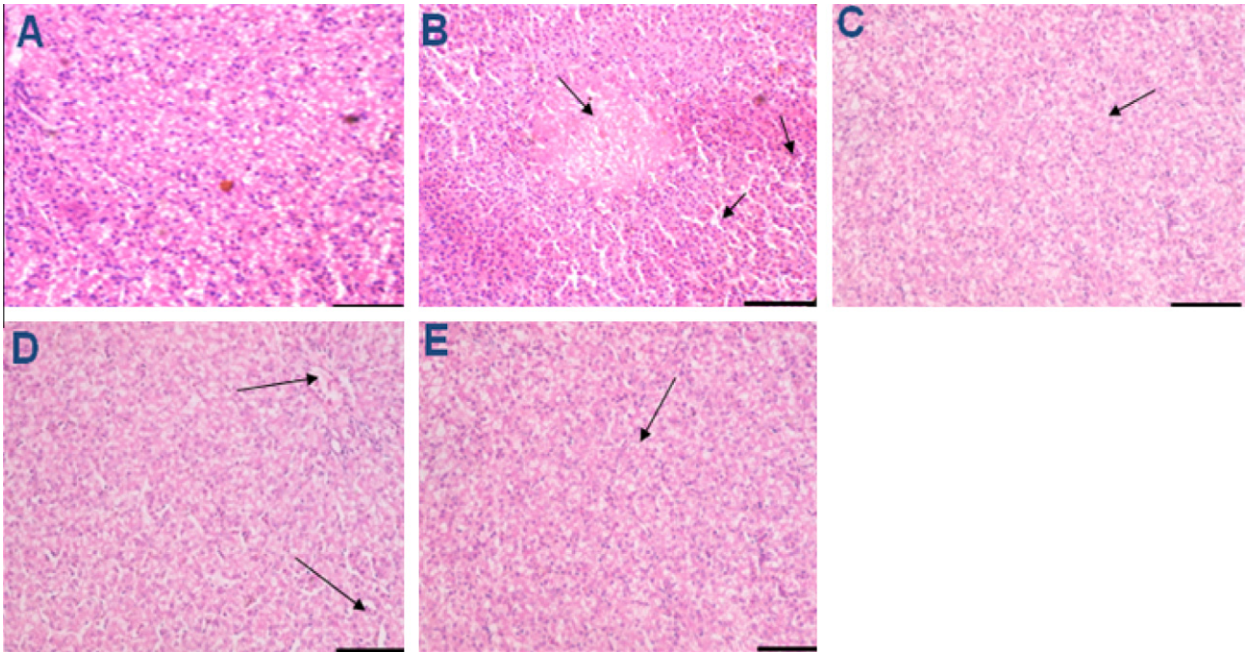

Fig. 9. (A) Photomicrograph of liver of control chicks showing normal histology. H and E: Lens 40×, (B) photomicrograph of liver of NDV infected chicks on 10 dpi, showing focal coagulation necrosis of parenchyma and degeneration of hepatocytes (arrows). H&E: Lens 40×, (C) photomicrograph of liver of NDV+**4b** treated chicks, showing cell regenerative process. H&E: Lens 40×, (D) photomicrograph of liver of NDV+**5b** treated chicks, showing necrosis and slight recovery process. H&E: Lens 40×, (E) photomicrograph of liver NDV+**6b** treated chicks, showing cells regenerative process as normalcy. H&E: Lens 40×. Scale bar = 10 μm.

results between the control group and experimental groups. Differences were considered significant when $P < 0.05$, $P < 0.001$. All the values were expressed as mean±S.D ($n = 6$). The Kaplan–Meier survival curves were applied by using R statistical software to assess the effects of title compounds **4b**, **5b**, **6b** on survival of NDV infected chicks, and the log-rank test was used to evaluate the differences in survival distributions.

Appendix A. Supplementary data

Supplementary data associated with this article can be found, in the online version, at http://dx.doi.org/10.1016/j.antiviral.2012.05.010.

References

Armitage, P., Allen, I., 1950. Methods of estimating the Ld-50 in quantal response data. Journal of Hygiene 48, 298–322.
Bossert, F., Vater, W., 1989. 1,4-Dihydropyridines-a basis for developing new drugs. Medicinal Research Reviews 9, 291–324.
Breitbart, M., Rohwer, F., 2005. Here a virus, there a virus, everywhere the same virus? Trends in Microbiology 13, 278–284.
Chemical Computing Group, 2002. Chemical Computing Group releases MOE version 2002.03. J. Chem. Educ. 79, 951–951.
Cho, H., Ueda, M., Shima, K., Mizuno, A., Hayashimatsu, M., Ohnaka, Y., Takeuchi, Y., Hamaguchi, M., Aisaka, K., Hidaka, T., et al., 1989. Dihydropyrimidines: novel calcium antagonists with potent and long-lasting vasodilative and antihypertensive activity. Journal of Medicinal Chemistry 32, 2399–2406.
Collins, M.S., Bashiruddin, J.B., Alexander, D.J., 1993. Deduced amino-acid-sequences at the fusion protein cleavage site of *Newcastle-Disease Viruses* showing variation in antigenicity and pathogenicity. Archives of Virology 128, 363–370.
Dastmalchi, S., Hamzeh-Mivehroud, M., Ghafourian, T., Hamzeiy, H., 2008. Molecular modeling of histamine H3 receptor and QSAR studies on arylbenzofuran derived H3 antagonists. Journal of Molecular Graphics and Modelling 26, 834–844.
Davies, R.J., Pierce, A.C., Forster, C., Grey, R., Xu, J., Arnost, M., Choquette, D., Galullo, V., Tian, S.K., Henkel, G., Chen, G., Heidary, D.K., Ma, J., Stuver-Moody, C., Namchuk, M., 2011. Design, synthesis, and evaluation of a novel dual FMS-like tyrosine kinase 3/stem cell factor receptor (FLT3/c-KIT) inhibitor for the treatment of acute myelogenous leukemia. Journal of Medicinal Chemistry 54, 7184–7192.
Edwards, R.A., Rohwer, F., 2005. Viral metagenomics. Nature Reviews Microbiology 3, 504–510.
Eisenberg, M.J., Brox, A., Bestawros, A.N., 2004. Calcium channel blockers: an update. American Journal of Medicine 116, 35–43.
Focher, F., Ubiali, D., Pregnolato, M., Zhi, C.X., Gambino, J., Wright, G.E., Spadari, S., 2000. Novel nonsubstrate inhibitors of human thymidine phosphorylase, a potential target for tumor-dependent angiogenesis. Journal of Medicinal Chemistry 43, 2601–2607.
Halliwell, B., Gutteridge, J.M.C., 1985. The importance of free-radicals and catalytic metal-ions in human-diseases. Molecular Aspects of Medicine 8, 89–193.
Han, S.Y., Sweeney, J.E., Bachman, E.S., Schweiger, E.J., Forloni, G., Coyle, J.T., Davis, B.M., Joullie, M.M., 1992. Chemical and pharmacological characterization of galanthamine, an acetylcholinesterase inhibitor, and its derivatives - a potential application in Alzheimers-disease. European Journal of Medicinal Chemistry 27, 673–687.
Huang, Z.H., Panda, A., Elankumaran, S., Govindarajan, D., Rockemann, D.D., Samal, S.K., 2004. The hemagglutinin–neuraminidase protein of *Newcastle disease virus* determines tropism and virulence. Journal of Virology 78, 4176–4184.
Kappe, C.O., 1998. 4-aryldihydropyrimidines via the Biginelli condensation: Aza-analogs of nifedipine-type calcium channel modulators. Molecules 3, 1–9.
Kappe, C.O., 2000. Recent advances in the Biginelli dihydropyrimidine synthesis. New tricks from an old dog. Accounts of Chemical Research 33, 879–888.
Kar, M., Mishra, D., 1976. Catalase, peroxidase, and polyphenoloxidase activities during rice leaf senescence. Plant Physiology 57, 315–319.
Khandazhinskaya, A.L., Shirokova, E.A., Skoblov, Y.S., Victorova, L.S., Goryunova, L.Y., Beabealashvilli, R.S., Pronyaeva, T.R., Fedyuk, N.V., Zolin, V.V., Pokrovsky, A.G., Kukhanova, M.K., 2002. Carbocyclic dinucleoside polyphosphonates: Interaction with HIV reverse transcriptase and antiviral activity. Journal of Medicinal Chemistry 45, 1284–1291.
Kokhan, O., Shinkarev, V.P., 2011. All-atom molecular dynamics simulations reveal significant differences in interaction between antimycin and conserved amino acid residues in bovine and bacterial bc(1) complexes. Biophysical Journal 100, 720–728.
Kornbrust, D.J., Mavis, R.D., 1980. Relative susceptibility of microsomes from lung, heart, liver, kidney, brain and testes to lipid peroxidation: correlation with vitamin E content. Lipids 15, 315–322.
Kumar, P., Khanna, M., Srivastava, V., Tyagi, Y.K., Raj, H.G., Ravi, K., 2005. Effect of quercetin supplementation on lung antioxidants after experimental influenza virus infection. Experimental Lung Research 31, 449–459.
Kumar, R., Semaine, W., Johar, M., Tyrrell, D.L.J., Agrawal, B., 2006. Effect of various pyrimidines possessing the 1-[(2-hydroxy-1-(hydroxymethyl)ethoxy)methyl] moiety, able to mimic natural 2'-deoxyribose, on wild-type and mutant hepatitis B virus replication. Journal of Medicinal Chemistry 49, 3693–3700.
Laskowski, R.A., 2001. PDBsum: summaries and analyses of PDB structures. Nucleic Acids Research 29, 221–222.

Machlin, L.J., Bendich, A., 1987. Free-radical tissue-damage-protective role of antioxidant nutrients. Faseb Journal 1, 441–445.
Misra, H.P., Fridovich, I., 1972. The role of superoxide anion in the autoxidation of epinephrine and a simple assay for superoxide dismutase. The Journal of Biological Chemistry 247, 3170–3175.
Morton, R.E., Evans, T.A., 1992. Modification of the bicinchoninic acid protein assay to eliminate lipid interference in determining lipoprotein protein content. Analytical Biochemistry 204, 332–334.
Nordberg, J., Arner, E.S.J., 2001. Reactive oxygen species, antioxidants, and the mammalian thioredoxin system. Free Radical Biology and Medicine 31, 1287–1312.
Ohkawa, H., Ohishi, N., Yagi, K., 1979. Assay for lipid peroxides in animal-tissues by thiobarbituric acid reaction. Analytical Biochemistry 95, 351–358.
Peterhans, E., 1997. Reactive oxygen species and nitric oxide in viral diseases. Biological Trace Element Research 56, 107–116.
Rajanarendar, E., Reddy, M.N., Murthy, K.R., Reddy, K.G., Raju, S., Srinivas, M., Praveen, B., Rao, M.S., 2010. Synthesis, antimicrobial, and mosquito larvicidal activity of 1-aryl-4-methyl-3,6-bis-(5-methylisoxazol-3-yl)-2-thioxo-2,3,6,10b-tetrahydro-1H-pyrimido[5,4-c]quinolin-5-ones. Bioorganic and Medicinal Chemistry Letters 20, 6052–6055.
Rao, V.K., Rao, A.J., Reddy, S.S., Raju, C.N., Rao, P.V., Ghosh, S.K., 2010. Synthesis, spectral characterization and biological evaluation of phosphorylated derivatives of galanthamine. European Journal of Medicinal Chemistry 45, 203–209.
Rao, V.K., Reddy, S.S., Krishna, B.S., Reddy, C.S., Reddy, N.P., Reddy, T.C.M., Raju, C.N., Ghosh, S.K., 2011. Design, synthesis and anti colon cancer activity evaluation of phosphorylated derivatives of lamivudine (3TC). Lett Drug Des Discov 8, 59–64.
Ravindra, P.V., Tiwari, A.K., Sharma, B., Rajawat, Y.S., Ratta, B., Palia, S., Sundaresan, N.R., Chaturvedi, U., Kumar, G.B.A., Chindera, K., Saxena, M., Subudhi, P.K., Rai, A., Chauhan, R.S., 2008. HN protein of *Newcastle disease virus* causes apoptosis in chicken embryo fibroblast cells. Archives of Virology 153, 749–754.
Santos, F.D., Abreu, P., Castro, H.C., Paixao, I.C.P.P., Cirne-Santos, C.C., Giongo, V., Barbosa, J.E., Simonetti, B.R., Garrido, V., Bou-Habib, D.C., Silva, D.D., Batalha, P.N., Temerozo, J.R., Souza, T.M., Nogueira, C.M., Cunha, A.C., Rodrigues, C.R., Ferreira, V.F., de Souza, M.C.B.V., 2009. Synthesis, antiviral activity and molecular modeling of oxoquinoline derivatives. Bioorganic and Medicinal Chemistry 17, 5476–5481.
Schwarz, K.B., 1996. Oxidative stress during viral infection: a review. Free Radical Biology and Medicine 21, 641–649.
Seal, B.S., King, D.J., Sellers, H.S., 2000. The avian response to *Newcastle disease virus*. Developmental and Comparative Immunology 24, 257–268.
Sherman, H., Kaplan, A.M., 1975. Toxicity studies with 5-bromo-3-sec-butyl-6-methyluracil. Toxicology and Applied Pharmacology 34, 189–196.
Sippl, W., 2002. Development of biologically active compounds by combining 3D QSAR and structure-based design methods. Journal of Computer-Aided Molecular Design 16, 825–830.
Walters, W.P., Murcko, A., Murcko, M.A., 1999. Recognizing molecules with drug-like properties. Current Opinion in Chemical Biology 3, 384–387.
Yu, B.P., 1994. Cellular defenses against damage from reactive oxygen species. Physiological Reviews 74, 139–162.